COMPARISON OF VORONOI BASED SCATTERED DATA INTERPOLATION SCHEMES

Tom Bobach
Geometric Algorithms Group / IRTG
University of Kaiserslautern, Germany

Martin Hering-Bertram
Computer Graphics Group
University of Kaiserslautern, Germany

Georg Umlauf
Geometric Algorithms Group
University of Kaiserslautern, Germany
email: {bobach,bertram,umlauf}@informatik.uni-kl.de

ABSTRACT

Voronoi based interpolation employs the concept of natural neighbors to define an interpolating function over discrete data known at scattered sample points. In this work we review the two main concepts for improving interpolation continuity inside the convex hull of the sample domain and compare four natural neighbor interpolants of C^1 and C^2 continuity. We give a visual presentation of all interpolants to provide insight into their overall behavior in addition to a comparison of their analytical and practical properties.

KEY WORDS

Scattered Data Interpolation, Voronoi Diagrams, Natural Neighbor Interpolation, Approximation Theory

1 Introduction

In nowadays scientific culture large amounts of unstructured sample data are generated in many applications, commonly as a result of numerical simulation or measure data from large scale sensor input. The common outcome is a collection of unstructured sample positions in the plane, in space or higher dimensions, where data has been calculated or measured. Processing this data requires a continuous, sometimes continuously differentiable representation. Under the assumption that the data has no noteworthy error to it, a continuous function must be found that interpolates the values at the sample positions, and matches higher order derivatives if they exist. A considerable body of work exists on the solution of the above problem. With the size of the data sets often exceeding the capacity of the processing computers, local interpolants become more and more important.

In this work we survey some spatial interpolation approaches based on natural neighbors, a concept derived from the Voronoi tessellation over a set of unstructured points. Natural neighbors inherently possess local support and cope well with inhomogeneous sampling densities. We review properties of existing methods and point out strengths and limitations of Voronoi-based interpolation.

1.1 Related Work

Natural neighbor coordinates were first introduced by Sibson [1, 2], who proposed a globally C^1-continuous interpolant in the plane that reproduces spherical quadratics. Farin extended this to an interpolant with second order precision on the basis of multivariate Béziersimplexes in [3]. Laplace coordinates, a simple identity provided by the structure of the Voronoi diagram, were presented by different authors in [4, 5, 6]. In [7] Hiyoshi et al. generalize Laplace and Sibson coordinates to natural neighbor coordinates of arbitrary continuity except at the data sites, called Standard coordinates. These are combined with Farin's approach by the same authors in [8] to produce a globally C^2 interpolant with cubic precision.

In the present work, we cover the following interpolants: Laplace, Sibson's, and Hiyoshi's coordinates in Section 3.1, 3.2, and 3.3, and Sibson's C^1, Farin's C^1, and Hiyoshi's C^2 interpolant in Section 4.3, 4.1, and 4.2.

For input data with values distributed along curves, transfinite interpolation is required. Gross et al. extended Sibson's coordinates to planar polygons [9], Hiyoshi et al. did so for Laplace coordinates in [6]. Transfinite interpolation to model discontinuities along line segments using is treated in [10]. In [11], Flötotto reviews most of the above methods in the more general setting of power diagrams and works out a C^1 interpolant that requires no knowledge of derivatives, following an idea of Clarkson [12]. Furthermore, she generalizes natural neighbor interpolation to point clouds on manifolds.

1.2 Outline

We summarize the concept of Voronoi diagrams in Section 2 to define local coordinates based on natural neighbors in Section 3. In Section 4, four interpolants of global C^1 and C^2 continuity are presented and discussed, along with the explanation of how to obtain arbitrary C^k continuity. A discussion of the presented schemes is given in Section 5. We conclude our presentation with an outlook on future work in Section 6.
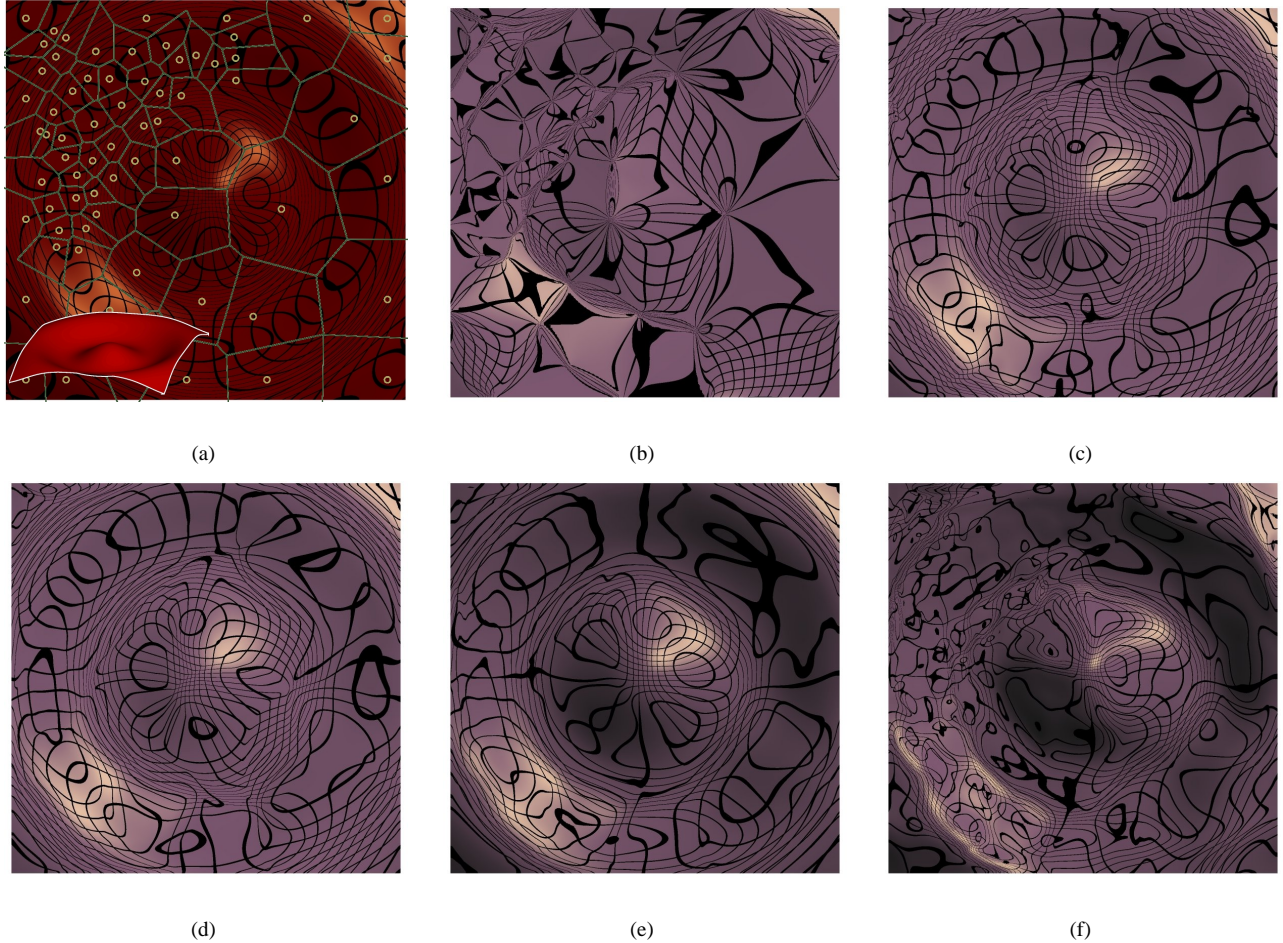
Figure 1. (a) the data was sampled from $\cos\|x\|$, note the inhomogeneous sampling density, (b) Standard coordinate interpolation, (c) Sibson's C^1, (d) Farin's C^1, (e) Hiyoshi's C^2, (f) squared Standard coordinates with gradient interpolation.

2 Voronoi Diagrams and Scattered Data

The overall problem of scattered data interpolation can be stated as follows: given sample sites $X = \{x_i\}_{i=1\ldots m} \subset \mathbb{R}^n$ and data values $Z = \{z_i\}_{i=1\ldots m} \subset \mathbb{R}$, find a function $f : \mathbb{R}^n \to \mathbb{R}$ that interpolates prescribed data at the sample points, $f(x_i) = z_i$. If derivatives are known at the sample positions, they are also subject to interpolation. We now explain how this relates to Voronoi diagrams.

Let X be generators for a Voronoi diagram, and $d(\cdot, \cdot)$ the Euclidean distance on $\mathbb{R}^n$. The resulting Voronoi diagram is the partition of space into convex tiles $\mathcal{T}_i = \{x \in \mathbb{R}^n | d(x, x_i) \leq d(x, x_j), i \neq j\}$. Two generators x_i and x_j are called *natural neighbors* if their associated tiles share a non-empty hyperface $s_{ij} := \mathcal{T}_i \cap \mathcal{T}_j$ with $(n{-}1)$-dimensional volume $\mathrm{vol}^{n-1}(s_{ij})$. To ensure boundedness of the elements of the Voronoi diagram, we will restrict our considerations to the interior $\mathcal{D}$ of the convex hull of X. We denote the set of indices of the natural neighbors for a generator x_i by N_i. If $n + 1$ or more tiles share a common point, the unique circumsphere through their generators is called *Delaunay sphere*, since it contains no other genera-

tor in its interior. For an overview on Voronoi diagrams the reader may refer to [13, 14].

Throughout the rest of this paper, $x_0 \in \mathcal{D}$ is an arbitrary, variable point for which we wish to interpolate its function value. Virtually inserting x_0 into X lets us reuse the notation from above. The set of neighbors N_0 depends on the position of x_0. Where it is unique, $f(x_0)$ is a rational C^∞-continuous function. Continuity issues arise whenever N_0 changes, i.e. when x_0 crosses a Delaunay sphere - see Section 3, and when x_0 passes another generator x_i - see Section 4. Separate treatment of the two cases is required for f to be globally C^k.

3 Generalized Local Coordinates

In the following, we consider the continuity of coordinate functions over $\mathcal{D} \setminus X$. Assume x_0 is expressed as a convex combination of its natural neighbors,

$$x_0 = \sum_{i \in N_0} \lambda_i x_i, \qquad \lambda_i \in \mathbb{R}^+.$$

(a)	(b)	(c)	(d)
(e)	(f)	(g)	(h)
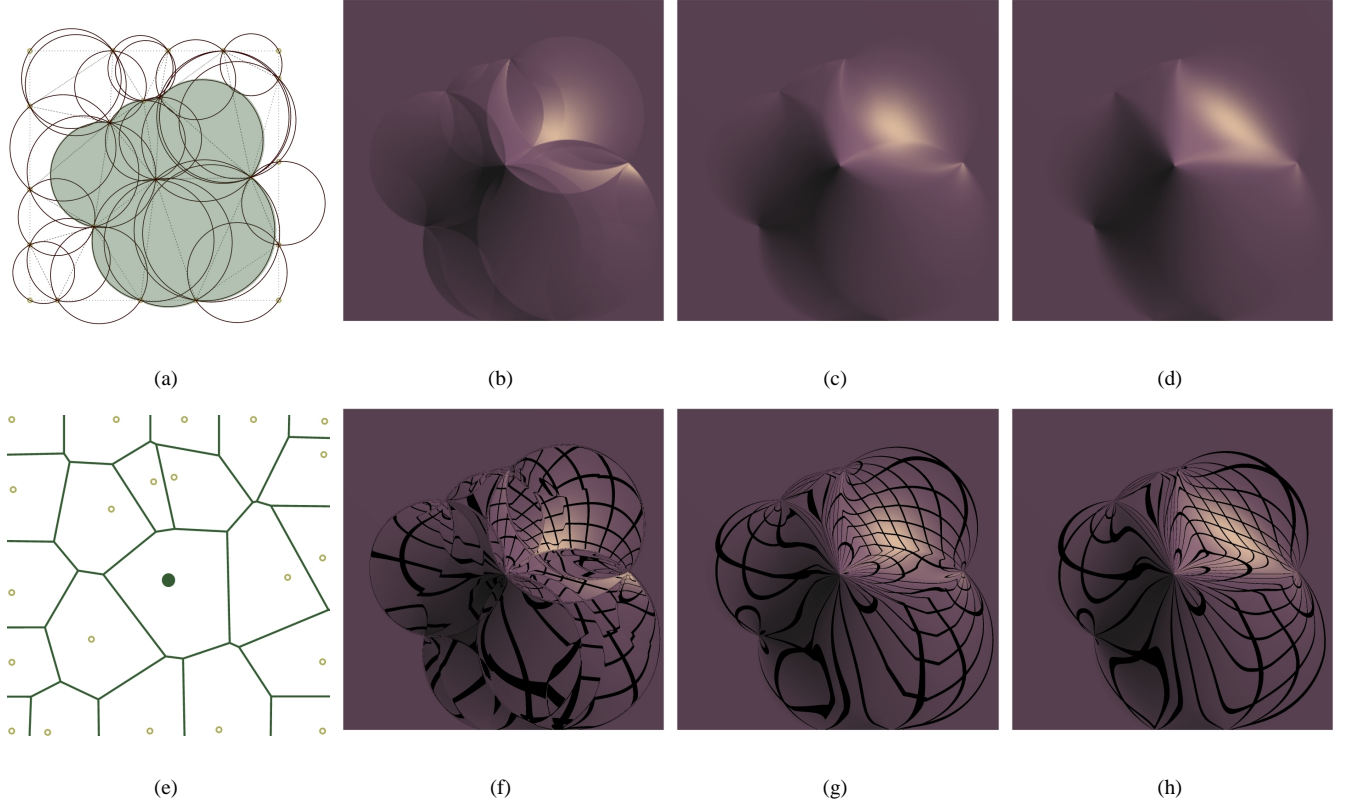
Figure 2. Visualization of the basis functions, all sample positions in (e) are set to zero except the solid one in the center. (a) shows the region of influence, (b)-(d) Laplace-, Sibson-, Standard-coordinates, (f)-(h) like above but with reflection lines to emphasize C^2-continuity.

In case $x_0 = x_i \in X$ we define $\lambda_i = 1$ and $N_0 = \{i\}$. This lets us define an interpolant by

$$f(x_0) = \sum_{i \in N_0} \lambda_i z_i. \tag{1}$$

Obviously, f is as smooth as λ_i. If $|N_0| > d+1$, $\{\lambda_i\}_{i \in N_0}$ is not uniquely determined. We look at different ways to construct local coordinates $\{\lambda_i\}_{i \in N_0}$ with different orders of continuity in $\mathscr{D} \setminus X$.

3.1 Laplace Coordinates

We first give C^0 local coordinates from [4, 5, 7], which we call Laplace coordinates in agreement with [7]. Let $s_i := \mathrm{vol}^{n-1}(s_{0i})$ be the volumes of the hyperfaces of $\mathscr{T}_0$ and $r_i := d(x_0, x_i)$. With $\tilde{\lambda}_i^0 = s_i / r_i$ the following identity holds

$$\sum_{i \in N_0} \tilde{\lambda}_i^0 x_0 = \sum_{i \in N_0} \tilde{\lambda}_i^0 x_i.$$

After normalization, we get local coordinates with C^0 continuity in $\mathscr{D} \setminus X$

$$\lambda_i^0 := \tilde{\lambda}_i^0 / \sum_{j \in N_0} \tilde{\lambda}_j^0.$$

The pieces of identical N_0 can be seen clearly in Figure 2(b,f) as the regions of smooth shading.

3.2 Sibson Coordinates

In the Voronoi diagram of $X \setminus \{x_0\}$, $\mathscr{T}_0$ occupies parts of its natural neighbors' tiles. The volumes $\tilde{\lambda}_i^1 = \mathrm{vol}^n(\mathscr{T}_i \cap \mathscr{T}_0)$ lead to the identity

$$\sum_{i \in N_0} \tilde{\lambda}_i^1 x_0 = \sum_{i \in N_0} \tilde{\lambda}_i^1 x_i$$

which was first observed by Sibson [1]. Normalization gives us

$$\lambda_i^1 := \tilde{\lambda}_i^1 / \sum_{j \in N_0} \tilde{\lambda}_j^1.$$

With this result, the corresponding scattered data interpolant from equation (1) was proposed in [2]. A close inspection of Figure 2(c,g) reveals the C^2 discontinuities, visible as sharp breaks in the reflection lines.

3.3 Standard Coordinates

A whole family of local coordinates, generalizing λ_i^0 and λ_i^1, with arbitrary smoothness in $\mathscr{D} \setminus X$, is given in [7].

The relationship stated there depends on the special structure of *power diagrams*. These are defined like Voronoi diagrams, but use a metric $d_p(\cdot, \cdot)$ that incorporates weights w_i attached to the generators, $\left(d_p(x, x_i)\right)^2 = \left(d(x, x_i)\right)^2 - w_i$. Note that if all w_i are equal, this gives the Voronoi diagram.

In [7] it is observed that for a fixed x_0, the shape of $\mathscr{T}_0$ in a power diagram can be controlled via a uniform power weight w on all generators in X and a weight of zero for x_0, see Figure 3(a). The face volumes s_i of $\mathscr{T}_0$ are piecewise polynomial functions in w, and so are $\tilde{\lambda}_i^0(w)$ in the power diagram. For $n = 2$, the s_i correspond to edge lengths and are piecewise linear in w. For $w = 0$, $\mathscr{T}_0(w)$ is the ordinary Voronoi tile, and shrinks for growing w until it completely disappears at $w = w_{max}$. Reversing the parameterization via $v = w_{max} - w$, the non-normalized local coordinates are recursively defined for $k \geq 0$ as

$$\tilde{\lambda}_i^k(u) = \int_0^u \tilde{\lambda}_i^{k-1}(w) \, dv,$$
$$\tilde{\lambda}_i^k = \tilde{\lambda}_i^k(w_{max}).$$

Normalization yields order k Standard coordinates

$$\lambda_i^k := \tilde{\lambda}_i^k / \sum_{j \in N_0} \tilde{\lambda}_j^k.$$

This procedure affects the order at which λ_i^k goes to zero. Thus, changes in the neighborhood N_0 lead to λ_i^k being continuous up to the k-th derivative. The difference to Sibson's original coordinates in Figure 2(g) is visible in Figure 2(h), where the reflection lines show no unsmooth behavior.

4 Interpolation Polynomials

In the previous section we reviewed methods to improve the continuity of local coordinates in $\mathscr{D} \backslash X$. For x_0 coinciding with a generator x_j, $\mathscr{T}_0$ no longer varies continuously with the position of x_0. Small perturbations of x_0 change the shape of $\mathscr{T}_0$ discontinuously and render the above approaches useless. For derivatives of $f(x_0)|_{x_0 \to x_j}$ of all adjoint pieces of f to agree, a polynomial in λ_i^k is used.

We first resketch the method proposed in [3]. The idea is based on the Bernstein-Bézier representation of simplices in l variables, see [15]. Let $\lambda^k = \{\lambda_i^k\}_{i \in N_0}$. The interpolant from equation (1) is identical to the linear Bézier simplex $b^1(\lambda^k)$ in $l = |N_0|$ variables with Greville abscissae located at the generators $\{x_i\}_{i \in N_0}$ and control points $\{z_i\}_{i \in N_0}$. By increasing the degree of the simplex, we get interior Bézier control points which can be chosen freely without interfering with the interpolation property. The directional derivatives $D_{x_j - x_i} b(\lambda)|_{x_0 = x_i}$ at the corners of the simplex are scaled differences of nearby control points. For $f(x_0)|_{x_0 = x_i}$ to be C^r, the mixed derivatives in all adjacent piecewise rational parts of f must agree up to order r. This fixes r layers of control points around the simplex corner in order to achieve C^r continuity at the generators.
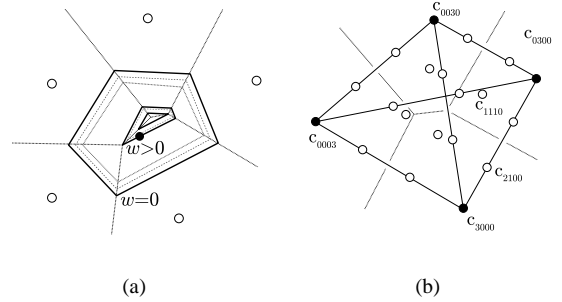
Figure 3. (a) Shape of $\mathscr{T}$ under different uniform power weights, (b) Cubic Bézier tetrahedron and its projected control net.

Note that already in case of cubic simplices, there are more control points than required for derivative modeling. These can be chosen arbitrarily without affecting continuity at x_i. It is, however, important to choose them carefully to prevent undesired oscillations in the interpolant.

Without loss of generality, let the elements of X be numbered such that $N_0 = \{1, \ldots, l\}$ and let $\alpha = (\alpha_1, \ldots, \alpha_l)$ be a multi index. The operator $\triangle_{ij}\alpha = (\ldots, \alpha_i - 1, \ldots, \alpha_j + 1, \ldots)$ takes us from α to its next neighbor in the control net in direction $x_j - x_i$, e.g. $\triangle_{12}(3, 0, 0, 0) = (2, 1, 0, 0)$ in Figure 3(b). By e^i and α^i we denote the i-th standard unit basis vector resp. the multi-index of the i-th corner of the simplex. The Bernstein-Bézier form of b^k with control points b_α is

$$b^k(x) = \sum_{|\alpha| = k} b_\alpha B_\alpha^k(x), \qquad x \in \mathbb{R}^l,$$
$$B_\alpha^k(x) = \frac{k!}{\alpha_1! \ldots \alpha_l!} x_1^{\alpha_1} \ldots x_l^{\alpha_l} = \frac{k!}{\alpha!} x^\alpha.$$

We will consider one approach using cubic simplices found in [3], and one based on quintic simplices as presented in [8].

4.1 Farin's Interpolant

The use of cubic Bézier simplices to interpolate first order derivatives at the generators is presented in [3]. Assume that the gradients $\mathbf{g}_i$ are given along with the data z_i. For $k = 3$, we get one layer of independent control points around each corner of the simplex b^3. Each is chosen to match the corresponding directional derivative for f. This means that the generator and all inner control points around it must be coplanar. We get

$$b_{\alpha^i} = z_i,$$
$$b_{\triangle_{ij}\alpha^i} = z_i + \frac{1}{3}(x_j - x_i)^T \mathbf{g}_i, \qquad i \neq j.$$

This fixes all control points except those on simplex faces, namely those having exactly three indices equal to one. By

(a)   (b)

(c)   (d)
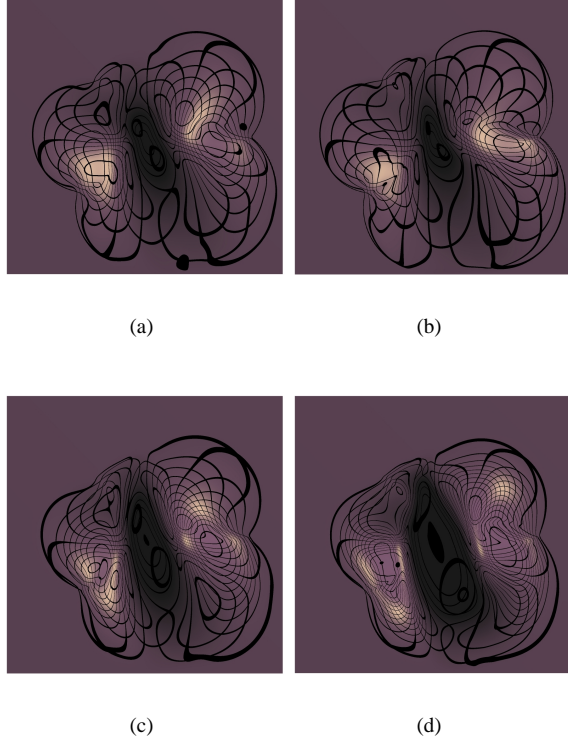
Figure 4. Reflection lines on a surface interpolating $z_i = 0$, $i = 1, \ldots, m$ and $\mathbf{g}_i = 0$, $i = 1, \ldots, m-1$ except for $\mathbf{g}_m = (1,0)^T$ at the center node as in Figure 2. (a) Sibson's C^1, (b) Farin's C^1, (c) Hiyoshi's C^2, (d) Squared Sibson's coordinates C^1.

degree elevation for Bézier simplices, these are chosen in a way that ensures quadratic precision of the resulting interpolant, see [3, 11]. Let $\beta = e^i + e^j + e^k$ for $i < j < k$, then b_β is an inner control point. Set $u = \frac{1}{3}(b_{\alpha^i} + b_{\alpha^j} + b_{\alpha^k})$ and $v = \frac{1}{6}\sum_{a,b \in \{i,j,k\}, a<b} b_{\triangle_{ab}\beta}$, the average of the remaining fixed control points, then $b_\beta = \frac{3}{2}v - \frac{1}{2}u$ yields quadratic precision for the interpolant. The resulting interpolant inherits C^1 continuity on $\mathscr{D} \setminus X$ from λ^1 and is given by

$$f(x_0) := b^3(\lambda^1).$$

Close inspection Figure 4(b) expose the C^2 discontinuities as corners in the reflection lines.

4.2 Hiyoshi's Interpolant

Applying the same approach as above to quintic Bézier simplices over λ^2, [8] present an explicit construction of control points that matches derivatives up to order two given in form of the *Hessian* $\mathbf{H}_i$ at generator x_i. Let i, j, k

be mutually distinct and $d_{ij} = x_j - x_i$, then

$$b_{\alpha^i} = z_i,$$
$$b_{\triangle_{ij}\alpha^i} = z_i + \frac{1}{5}\mathbf{g}_i^T d_{ij},$$
$$b_{\triangle_{ij}\triangle_{ij}\alpha^i} = z_i + \frac{2}{5}\mathbf{g}_i^T d_{ij} + \frac{1}{20}d_{ij}^T \mathbf{H}_i d_{ij},$$
$$b_{\triangle_{ij}\triangle_{ik}\alpha^i} = z_i + \frac{1}{5}\mathbf{g}_i^T d_{ij} + \frac{1}{20}d_{ij}^T \mathbf{H}_i d_{ij},$$
$$\ldots$$

The remaining control points are again chosen based on the principle of degree elevation to ensures cubic precision. For more details we refer to [8]. The smooth reflection lines in Figure 4(c) indicate C^2 continuity of the surface.

4.3 Sibson's Interpolant

Another way of setting up a polynomial in λ^1 was proposed in [2], giving a C^1 function interpolating predefined gradient information and reproducing spherical quadratics. Its construction is based on λ^1 and does not generalize easily to higher degrees of continuity. The proposed C^1 interpolant is a combination of Sibson's C^0 interpolant $f^1(x_0) := \sum_{i \in N_0} \lambda_i^1 x_i$ and an interpolant ζ that blends first order functions. Let $r_i = d(x_0, x_i)$, $\gamma_i = \lambda_i^1/r_i$, then

$$\zeta_i = z_i + (x_0 - x_i)^T \mathbf{g}_i,$$
$$\zeta = \left(\sum_{i \in N_0} \gamma_i \zeta_i\right)\Big/\left(\sum_{i \in N_0} \gamma_i\right).$$

With

$$\alpha = \left(\sum_{i \in N_0} \lambda_i^1 r_i\right)\Big/\left(\sum_{i \in N_0} \gamma_i\right),$$
$$\beta = \sum_{i \in N_0} \lambda_i^1 (r_i)^2,$$

f^1 and ζ are combined to yield Sibson's C^1 interpolant

$$f(x_0) = (\alpha f^1(x_0) + \beta\zeta)/(\alpha + \beta).$$

Similar to Farin's method, corners in the reflection lines in Figure 4(a) indicate C^2 discontinuities.

4.4 Squared Coordinates

In the above methods a polynomial in the local coordinates was set up in a sophisticated way to interpolate derivative data. As mentioned before, to ensure C^1 continuity at x_i, the first derivatives of $f(x_0)$ have to agree. This is trivially satisfied for vanishing derivatives. Taking the second power of λ_i^k, its first derivatives consequently those of $f(x_0)|_{x_j}$ vanish. Let

$$\tilde{\lambda}_i^k = (\lambda_i^k)^2\Big/\sum_{j \in N_0} (\lambda_j^k)^2.$$

We can now impose any gradient at the generators by blending first order functions using $\tilde{\lambda}_i^k$

$$f(x_0) = \sum_{i \in N_0} \tilde{\lambda}_i^k \left(z_i + \mathbf{g}_i^T(x_0 - x_i)\right).$$

Interpolant	$D \setminus X$	X	Prec.	Der. req	Gener.
Laplace	C^0	C^0	P^1		no
Sibson C0	C^1	C^0	P^1		no
Standard	C^k	C^0	P^1		yes
Sibson C1	C^1	C^1	s.q.*	$\mathbf{g}$	no
Farin	C^1	C^1	P^2	$\mathbf{g}$	yes
Squared	C^1	C^1	P^2	$\mathbf{g}, \mathbf{H}$	yes
Hiyoshi	C^2	C^2	P^3	$\mathbf{g}, \mathbf{H}$	yes

Table 1. Continuity, precision, derivative requirements, and the ability to generalize to higher degrees of smoothness. *spherical quadratics.

This can be extended to interpolate derivatives of arbitrary degree, although at the expense of lacking smoothness despite of continuity as can be seen in Figure 4(d).

5 Discussion and Comparison

We now compare the interpolants based on natural neighbor and second degree Standard coordinates. These interpolants have a number of analytically provable properties, summarized in Table 1.

We have implemented all the above methods and give a visual comparison for the same sample problem Sibson used in [2]. As seen in Figure 1 and 5 (a), the data is sampled from the functional $cos\|x\|$, with higher sample density in the upper-left corner.

Farin's and Hiyoshi's methods have quadratic respective cubic polynomial precision, Sibson's method recovers spherical quadratics. They can be expected to perform well on sample data derived from polynomials of similar degree, which motivates our choice of the non-polynomial sample data set.

We choose second order Standard coordinates to represent the non-modified local coordinate interpolants and depict their low approximation quality. It can clearly be seen in Figure 1 and 5(b) that even though being C^2-continuous almost everywhere, the interpolant based on Standard coordinates is not suited for interpolation of the sample data. This comes as no big surprise but gives a very good motivation for the additional efforts one has to put into establishing continuity at the sample points.

For the gobally C^1 methods including Hiyoshi's, the visual difference between Figure 1 and 5(c-e) is not as obvious, yet Farin's interpolant appears somewhat superior to both Sibson's original C^1 interpolant and Hiyoshi's C^2 interpolant. Considering the complexity of the above approaches, it is tempting to resort to simpler methods like the squared Sibson's coordinates. However, the poor performance of this interpolant in Figure 1 and 5(f) despite its analytical properties makes it inappropriate in most applications. We include this approach into our comparison disregarding its shortcomings to show that analytic properties of the interpolant are insufficient to make it well-behaved in user perception.

Extension to higher dimensions Since neither the Voronoi diagram, the multivariate Bernstein-Bézier representation nor any presented procedure to derive natural neighbor coordinates is restricted in dimension, these approaches can be extended to three or more dimensions in a straigthforward way. In doing so, however, one will face difficulties that emerge naturally from the growing complexity of the problem. Furthermore, Bézier simplex approach can be applied to any kind of local, convex barycentric coordinates.

Extension to higher continuity Of the methods considered in this work, only the combination of Standard coordinates s^k with Bernstein-Bézier-polynomials can be generalized to higher continuity in a straightforward way. But we must stress that computational complexity as well as implementation rapidly become infeasible. Even in the two-dimensional setting, construction of the Béziercontrol net from second order derivatives becomes a bottleneck if the number of natural neigbors is high, e.g. $|N_0| > 20$.

6 Conclusion

We have given an overview of natural neighbor interpolation schemes, focused on Sibson's, Farin's, and Hiyoshi's globally C^1, C^1, and C^2-continuous schemes. The two main ingredients in a globally C^k interpolant have been summarized, i.e. the construction of local coordinates and the setup of suitable polynomials in the sample positions.

The visual comparison provided insight into the behaviour of the schemes in a setting with inhomogeneous sampling densities. Furthermore, reflection lines have been applied to visualize the smoothness of the gradient, yielding better insight than the usual shading for comparison of C^1 and C^2 continuity.

Future research will focus on the automatic estimation of derivatives, since especially for measurement data, derivatives are seldom given.

Acknowledgements

References

[1] R. Sibson. A vector identity for the dirichlet tessellation. *Mathematical Proceedings of Cambridge Philosophical Society*, 87:151–155, 1980.

[2] R. Sibson. A brief description of natural neighbor interpolation. *Interpreting Multivariate Data*, pages 21–36, 1981.
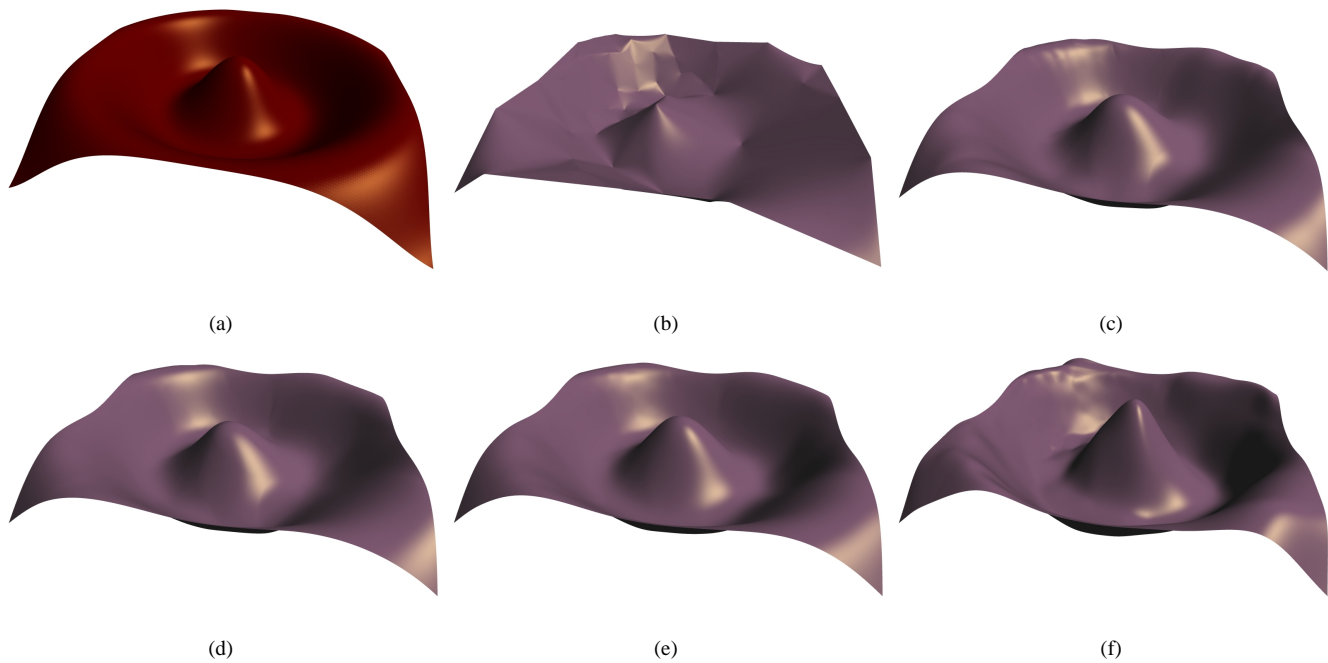
Figure 5. (a) $\cos \|x\|$, (b) Standard coodinate interpolation, (c) Sibson's C^1, (d) Farin's C^1, (e) Hiyoshi's C^2, (f) squared Standard coordinates with gradient interpolation.

[3] Gerald Farin. Surfaces over Dirichlet Tessellations. *Computer Aided Geometric Design*, pages 281–292, Jun 1990.

[4] N. H. Christ, R. Friedberg, and T. D. Lee. Weights of links and plaquettes in a random lattice. *Nuclear Physics B*, 210(3):337–346, 1982.

[5] V. V. Belikov, V. D. Ivanov, V. K. Kontorovich, S. A. Korytnik, and A. Yu. Semenov. The non-Sibsonian interpolation: A new method of interpolation of the values of a function on an arbitrary set of points. *Computational Mathematics and Mathematical Physics*, 37(1):9–15, 1997.

[6] Hisamoto Hiyoshi and Kokichi Sugihara. An interpolant based on line segment voronoi diagrams. In *JCDCG*, pages 119–128, 1998.

[7] Hisamoto Hiyoshi and Kokichi Sugihara. Voronoi-based interpolation with higher continuity. In *Symposium on Computational Geometry*, pages 242–250, 2000.

[8] Hisamoto Hiyoshi and Kokichi Sugihara. Improving the global continuity of the natural neighbor interpolation. In *ICCSA (3)*, pages 71–80, 2004.

[9] Lee Gross and Gerald E. Farin. A transfinite form of Sibson's interpolant. *Discrete Applied Mathematics*, 93:33–50, 1999.

[10] F. Anton, D. Mioc, and C. Gold. Line Voronoi diagram based interpolation and application to digital terrain modelling. In *ISPRS - XXth Congress, Vol.2*. International Society for Photogrammetry and Remote Sensing, 2004.

[11] Julia Flötotto. *A coordinate system associated to a point cloud issued from a manifold: definition, properties and applications*. PhD thesis, Université de Nice-Sophia Antipolis, Sep 2003.

[12] Kenneth L. Clarkson. Convex hulls: Some algorithms and applications. Presentation at Fifth MSI-Stony Brook Workshop on Computational Geometry, 1996.

[13] Franz Aurenhammer. Voronoi diagrams - a survey of a fundamental geometric data structure. *ACM Computing surveys*, 23(3):345–405, 1991.

[14] Atsuyuki Okabe, Barry Boots, Kokichi Sugihara, and Sung Nok Chiu. *Spatial Tessellations: Concepts and applications of voronoi diagrams*. Wiley series in probability and statistics. John Wiley & Sons Ltd, 2nd edition, 2000.

[15] Carl de Boor. B-form basics. *Geometric Modelling - Algorithms and New Trends*, pages 131–148, 1987.